JOURNAL OF CHEMICAL & ENGINEERING DATA

ARTICLE

pubs.acs.org/jced

Adsorption of Anionic Dyes on Boron Industry Waste in Single and Binary Solutions Using Batch and Fixed-Bed Systems

Necip Atar,[†,‡] Asim Olgun,[‡] Shaobin Wang,*[,†] and Shaomin Liu[†]

[†]Department of Chemical Engineering, Curtin University of Technology, GPO Box U1987, Perth, WA 6845, Australia

[‡]Department of Chemistry, University of Dumlupinar, Kutahya, Turkey

ABSTRACT: The removal of Acid Red 183 (AR183) and Reactive Blue 4 (RB4) from single and binary solutions onto a waste material (WM) from the boron industry was studied. The adsorption capacities of AR183 and RB4 on WM in single dye solutions were found to be $9.11 \cdot 10^{-5}$ mol·g^{-1} and $7.33 \cdot 10^{-5}$ mol·g^{-1}, respectively. Because of competitive adsorption, the adsorption capacities in binary solutions were reduced to $7.43 \cdot 10^{-5}$ mol·g^{-1} and $6.37 \cdot 10^{-5}$ mol·g^{-1}, respectively. The adsorption followed pseudosecond-order kinetics, and the isotherm fit well to the Langmuir model. In column experiments, the adsorption of dyes from single and binary solutions was fit well by the Thomas model. The breakthrough and exhaustion capacity of each dye decreased with increasing flow rate and decreaed in the presence of the other dye. The thermodynamic parameters such as Gibbs energy change (ΔG), entropy change (ΔS), and enthalpy change (ΔH) were obtained, showing the exothermic nature of dye adsorption on WM.

INTRODUCTION

The contamination of water by dye stuffs has been recognized as an issue of growing importance in recent years. Decolorization of wastewater has become one of the major tasks in wastewater treatment. Many industries currently use a variety of dyes to color their products, for example, in the textile, rubber, paper, plastics, leather, cosmetics, food, and mineral processing industries.[1−5] There are several methods to treat dye-contaminated effluents such as adsorption,[6] coagulation,[7] chemical oxidation,[8−10] membrane filtration,[11] and anaerobic treatment.[12] Adsorption is a simple and cost-effective technique and is widely used in industry. The removal of dyes from textile wastewater has considered the adsorption process as an important application using low-cost adsorbents against expensive ones like activated carbon.[13−17] In recent years, waste materials (WMs) have been used as low cost adsorbents such as agricultural wastes,[18] red mud,[5,19] fly ash,[20,21] blast furnace slag,[22] natural zeolite,[23] and fertilizer waste.[24] In an earlier study,[25] a boron industry waste has also been tested in the adsorption of basic dyes from aqueous solution.

Boron ores are one of the most important underground natural resources of Turkey. During the enrichment process of boron ores, a large quantity of boron waste is discharged into waste dams near the plant area. This will cause an important environmental problem. The boron WM contains colemanite, ulexite, zeolite, and some clays. Colemanite ($Ca_2B_6O_{11}•5H_2O$) is a borate mineral with a basic structure containing endless chains of interlocking $BO_2(OH)$ triangles and $BO_3(OH)$ tetrahedrons with the calcium, water molecules, and extra hydroxides interspersed between the chains. Ulexite ($NaCaB_5O_9•8H_2O$) is a structurally complex mineral that contains chains of sodium, water, and hydroxide octahedra. The chains are linked together by calcium, water, hydroxide, and oxygen polyhedra and massive boron units. The boron units have a formula of $B_5O_6(OH)_6$ and a charge of −3 and are composed of three borate tetrahedra and two borate triangular groups. Colemanite ore waste[26] and boron waste[27] are excellent adsorbents for the removal of basic and acid dyes from single dye solutions in a batch system. For textile wastewater, reactive dyes are the most widely used, and these dyes are highly resistance to biodegradation. The removal of reactive dyes is vitally important in dye containing water treatment.

The adsorption capacity obtained from a batch system is useful in providing the fundamental information regarding the effectiveness of adsorption. Batch systems are not likely to be employed in industries. A fixed-bed system is more useful for textile wastewater treatment from industrial sources. Although real wastewater contains multidye effluents, there are only limited studies on multidye adsorption in both column and batch systems.[28,29]

The objective of the present study is to investigate the adsorption of acid and reactive dyes onto a WM containing boron impurities from single and binary dye solutions in batch and fixed-bed systems. The kinetics, adsorption isotherm, and thermodynamics were studied for an in-depth understanding of dye adsorption characteristics.

EXPERIMENTAL SECTION

Adsorbent Material, Dyes, and Characterization. The WM used in this study was obtained from Etibor (Bigadiç Balıkesir, Turkey) without any chemical or physical treatment. Acid Red 183 (AR183, CI 18800, MW = 584.87 g·mol^{-1}) and Reactive Blue 4 (RB4, CI 61205, MW = 637.43 g·mol^{-1}) were purchased from Sigma-Aldrich. The chemical structures of the AR183 and RB4 are given in Figure 1.

The chemical structure and phases of WM were determined by an X-ray diffractogram using a Rigaku miniflex diffractometer with Cu Kα radiation over a range (2θ) of 5° to 60° scanning at 30 kV and 15 mA. The chemical composition of WM was

Received: October 5, 2010
Accepted: January 3, 2011
Published: January 18, 2011

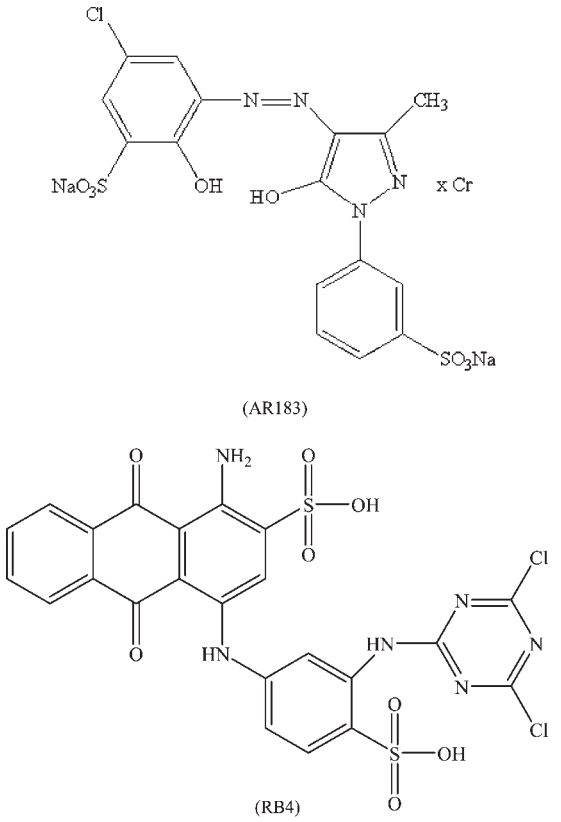

Figure 1. Chemical structure of AR183 and RB4.

obtained using a X-ray fluorescence (XRF) spectrometer (ARL FISON).

Zeta potential measurements were conducted using a zeta meter 3.0 over a broad range of pH (3 to 9). A known amount of WM was suspended in 50 mL of distilled water, and the solution pH was adjusted between 3.0 and 9.0 using either 0.1 M HCl (Sigma-Aldrich) or 0.1 M NaOH (Sigma-Aldrich) solutions. After pH adjustment, the mixtures were equilibrated with a magnetic stirrer for 20 min, and the zeta potential was measured.

Batch Adsorption Studies. The dye stock solutions were prepared at a concentration of 1000 $mg \cdot L^{-1}$, and the experimental solutions were obtained by diluting the stock solution with Milli-Q water. Batch experiments were carried out in 50 mL flasks at 298 K in an isothermal shaker with a mixing speed of 200 rpm to investigate the effects of operating conditions (pH, adsorbent dosage, contact time, and initial dye concentration). For single dye adsorption, the concentration of dye solution was analyzed using a UV−vis spectrophotometer (Spectronic 20 Genesis, USA) at preset time intervals. Earlier the wavelength at which the maximum absorbance λ_{max} (nm) occurred for each dye in aqueous solution was determined by performing full range [(200 to 900) nm] wavelength scans. The maximum absorbance (λ_{max}, nm) of AR183 and RB4 was observed at (496 and 595) nm, respectively. Concentrations of dye solution were then estimated quantitatively using the linear regression equations obtained by plotting a calibration curve for each dye over a wide range of concentrations. In a binary system with components A and B, the measurement would be carried out at their maximum absorbance wavelength $\lambda_{1,max}$ and $\lambda_{2,max}$, respectively, giving absorbances of A_1 and A_2. The dye concentration of the particular component could be determined by the following equations:[30]

$$C_A = \frac{k_{B_2}A_1 - k_{B_1}A_2}{k_{A_1}k_{B_2} - k_{A_2}k_{B_1}} \quad (1)$$

$$C_B = \frac{k_{A_1}A_2 - k_{A_2}A_1}{k_{A_1}k_{B_2} - k_{A_2}k_{B_1}} \quad (2)$$

where k_{A1}, k_{B1}, k_{A2}, and k_{B2} are the calibration constants for components A and B at wavelength $\lambda_{1,max}$ and $\lambda_{2,max}$, respectively. For binary dye solutions, initial dye concentrations were maintained at 1:1 (w/w).

To investigate the effect of pH, the solution pH was adjusted between 3 and 9 using 0.1 M HCl or NaOH solutions and measured by a pH meter (Radiometer PHM250 ion analyzer). The pH experiments were performed by shaking the solutions for 60 min at 298 K, with 50 mg of WM in 50 mL of dye solution at different pH levels. Isothermal and kinetic studies were conducted at 298 K, whereby 50 mg of WM was kept in contact with 50 mL of dye solution of varying concentrations [(25 to 250) $mg \cdot L^{-1}$] at different time intervals [(10 to 200) min] at pH 3. The batch experiments of binary dye solutions were carried out using a similar procedure as described above.

Column Adsorption Studies. Column adsorption experiments were carried out to investigate the effect of flow rate on the adsorption of AR183 and RB4 on WM in both single and binary dye solutions and to compare the adsorption capacities with a batch system. The fixed-bed column studies were performed in a glass column made of 1 cm inner diameter and 12 cm height. A stainless steel sieve was attached at the bottom of column with a layer of glass wool. A known quantity of WM was then packed in the column to yield a bed height of 6 cm. Dye solution was fed in an up-flow manner through the column at a desired flow rate [(1, 3, and 5) $mL \cdot min^{-1}$] using a peristaltic pump. Effluent samples were collected at the outlet of the column at different time intervals and analyzed for dye concentration. All fixed-bed studies were carried out at a constant inlet dye concentration of 100 $mg \cdot L^{-1}$, initial solution pH of 3, and 298 K. The breakthrough curves were obtained by plotting the ratio (C/C_o) of dye concentration (C) at time t to initial concentration (C_0) versus time (t) at different flow rates.

RESULTS AND DISCUSSION

Characteristics of Adsorbent. The properties of the WM used in this study were characterized by XRF (ARL FISON), X-ray diffraction (Rigaku miniflex diffractometer), and zeta potential measurements (Zeta Meter 3.0). The chemical composition of the WM is presented in Table 1. As seen the composition of the WM contains the elements boron, silicon, calcium, and magnesium. The XRD analysis of WM given in Figure 2 reveals the major mineral phases, namely, colemanite, ulexite, and zeolite. The zeta potential, which corresponds to the surface charge of a solid, is one of the most essential factors influencing the adsorption process. The zeta potential measurements of WM determined at various pH values is presented in Figure 3. As shown, the surface of the WM has a positive charge in the range of pH < 4.02. The surface of WM in the range of pH > 4.02 exhibited a negative charge mainly due to the variable charge from surface hydroxyl sites. The oxygen atoms present on the WM surface interact with water in an acidic medium. In an acidic medium, the surface of WM

dx.doi.org/10.1021/je100993m |J. Chem. Eng. Data 2011, 56, 508–516

becomes positively charged favoring anionic dye uptake. The mechanism for the adsorption of the anionic dyes from aqueous solution is shown in Scheme 1.

Batch Studies. *Effect of pH.* In the batch process of both single and binary dye solutions, the effect of pH on the adsorption was investigated by varying the pH over a range of 3 to 9. The initial dye concentration (100 $mg \cdot L^{-1}$), adsorbent dosage (1 $g \cdot L^{-1}$), and contact time (60 min) were kept constant. Figure 3 shows the effect of pH on the adsorption of AR183 and RB4 on WM from both single and binary dye solutions. As seen, the pH is an important controlling parameter in the batch adsorption process. The uptake levels of the dyes in both single and binary dye solutions were reduced significantly with increasing pH from 3 to 9. In the single systems, the adsorption capacities of AR183 and RB4 were obtained as $7.68 \cdot 10^{-5}$ $mol \cdot g^{-1}$ and $6.05 \cdot 10^{-5}$ $mol \cdot g^{-1}$, respectively, at a pH of 3. The maximum positive zeta potential value of WM was recorded at a pH of 3.0, which represented the maximum adsorption efficiency of the anionic dyes. Because of electrostatic attractions between negatively charged dye molecules and the positively charged surface of WM, the adsorption capacity of WM increased as the solution pH decreased. Similar results were observed for the binary dye systems. In the binary system, because of the high degree of competition on active sites between the two types of dye molecules, the adsorption capacities of AR183 and RB4 were reduced to $4.91 \cdot 10^{-5}$ $mol \cdot g^{-1}$ and $3.21 \cdot 10^{-5}$ $mol \cdot g^{-1}$, respectively, at a pH of 3.0. Hence, the solution pH of 3.0 was chosen as the optimum pH in the following batch studies.

Since the WM contains a significant amount of boron impurity, the boron concentration in the solution after the adsorption test was analyzed using a ICP-MS (inductively coupled plasma-mass spectrometry, Perkin-Elmer 9000), and it was observed that the boron concentration in the solution was below 0.5 $mg \cdot L^{-1}$ for the two adsorption systems at pH of 3. The boron concentration was within the limit of the standard for the water discharged to the environment.[31]

Effect of Adsorbent Dosage and Contact Time. The effect of adsorbent mass on dye adsorption was investigated for both single and binary systems. The dye uptake was observed to increase as the dosage increased up to a dosage of 1 $g \cdot L^{-1}$ (figure not shown). A series of contact time experiments were conducted at different times [(10 to 200) min] with a constant initial dye concentration of 100 $mg \cdot L^{-1}$, adsorbent dosage of 1 $g \cdot L^{-1}$, pH of 3, and 298 K for the two dyes. Figure 4 shows the effect of contact time on the adsorption of AR183 and RB4 from single and binary dye solutions. Since a large number of vacant surface sites were available for the adsorption in the initial stage, the adsorption of dyes was rapid and increased with increasing time up to 60 min. After this period, the adsorption leveled off and was virtually constant. Since AR183 has a lower molecular weight than that of RB4, the uptake level of AR183 is higher than RB4 for both systems at the equilibrium time. A comparison of the single and binary systems shows that the contact time curves for the binary system were a similar shape of those in the single system and the adsorption

Table 1. Chemical Compositions of Boron Industry Waste

	chemical analysis (% by weight)
SiO_2	15.50
Al_2O_3	0.49
Fe_2O_3	0.28
CaO	17.52
MgO	10.32
SO_3	14.20
Na_2O	7.52
K_2O	0.38
B_2O_3	13.37
loss on ignition	20.42

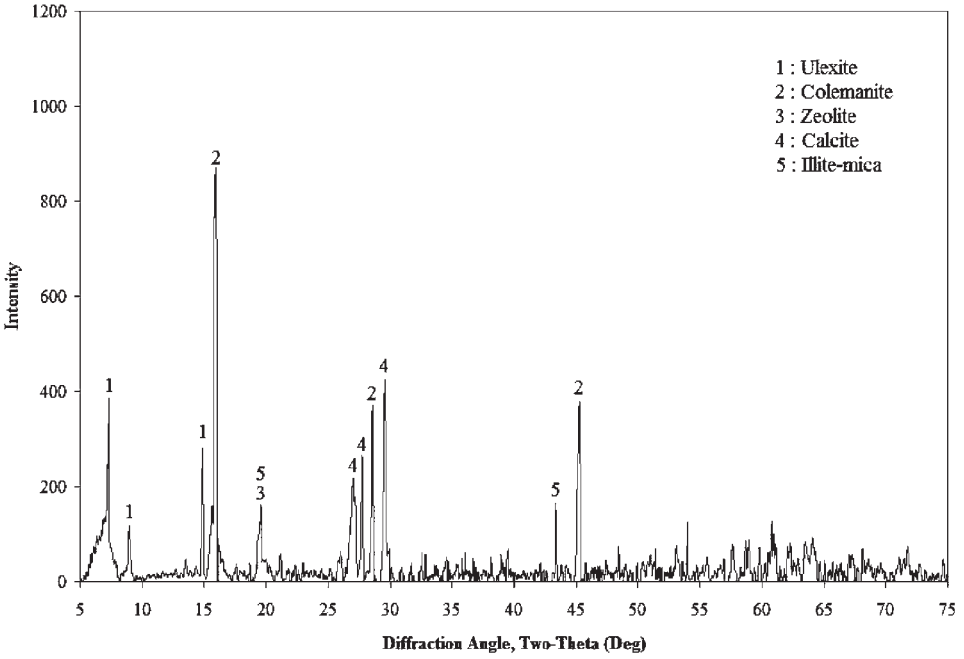

Figure 2. XRD patterns of WM.

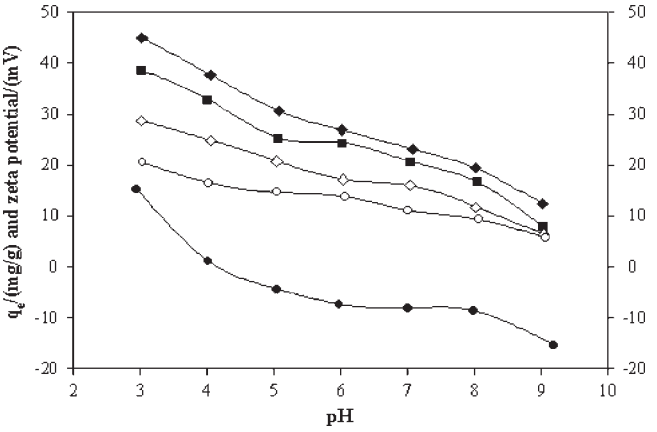

Figure 3. Effect of pH on the adsorption of AR183 and RB4 from single and binary solutions [initial dye concentration C_o = 100 mg·L^{-1} (single system), C_o = (100 mg AR183+ 100 mg RB4)/L (binary system), T: 298 K, adsorbent dosage: 1 g·L^{-1}, contact time: 60 min; agitation speed: 200 rpm] and ζ potential values of adsorbent at various pH values. [-●-, zeta potential; -◆-, AR183 (single system); -■-, RB4 (single system); -◇-, AR183 (with RB4); -○-, RB4 (with AR183)].

Scheme 1. Mechanism of the Anionic Dye Adsorption on WM

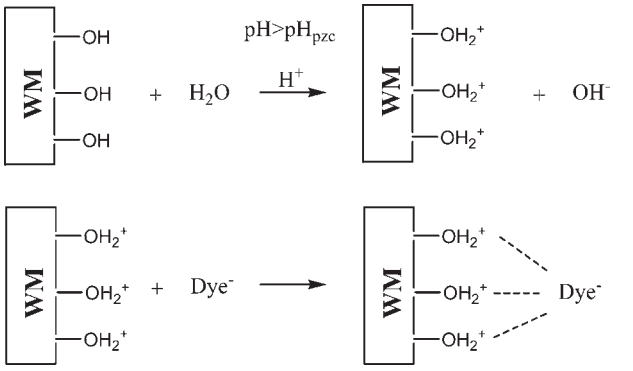

capacities of the dyes in the binary system were lower than the uptakes of the dyes in the single system. This can be attributed to competitive adsorption (the interaction between the dyes in the adsorbed phase), and the dyes compete with each other to occupy the same binding sites.

Adsorption Kinetics. To design a wastewater treatment for textile industrial plants, it is important to predict the rate of adsorption. In this study, two kinetic models were used to fit the experimental data. The Lagergren pseudofirst-order model is expressed by the following equation;[32]

$$\log(q_e - q_t) = \log q_e - (k_1/2.303)t \quad (3)$$

where q_e is the adsorption equilibrium capacity (mol·g^{-1}), q_t is the amount of dye adsorbed (mol·g^{-1}) at time t, and k_1 is the pseudofirst-order rate constant (min^{-1}). To obtain k_1 and q_e from Figure 4, we can use the following equation for curve fitting of the first-order kinetics.

$$q_t = q_e(1 - \exp(-k_1 t)) \quad (4)$$

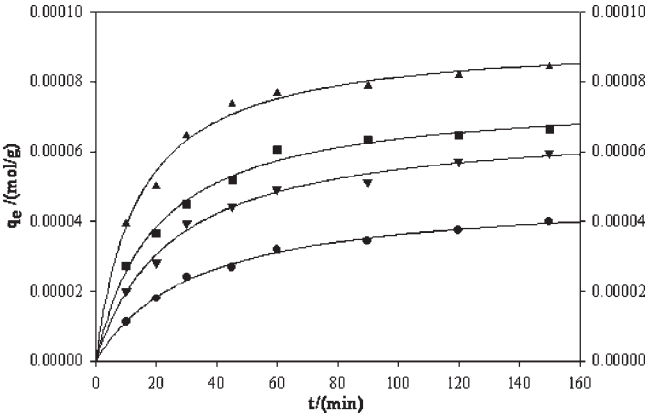

Figure 4. Adsorption kinetics and the effect of contact time on the adsorption of AR183 and RB4 from single and binary solutions [pH: 3; initial dye concentration C_o = 100 mg·L^{-1} (single system), C_o = (100 mg AR183 + 100 mg RB4)/L (binary system), T: 298 K, adsorbent dosage: 1 g·L^{-1}; agitation speed: 200 rpm; ▲, AR183 (single system); ■, RB4 (single system); ▼, AR183 (with RB4); ●, RB4 (with AR183); —, pseudosecond-order kinetic model].

The integral form of the pseudosecond-order model is given by the following equation;[33]

$$\frac{t}{q_t} = \frac{1}{k_2 q_2^2} + \frac{1}{q_2} t \quad (5)$$

where q_2 is the maximum adsorption capacity (mol·g^{-1}); k_2 is the rate constant of the pseudosecond-order equation (g·mol^{-1}·min^{-1}); q_t is the amount of dye adsorbed per unit mass of the adsorbent (mol·g^{-1}). The nonlinear form of eq 5 can be given by the following equation;

$$q_t = \frac{q_2^2 k_2 t}{1 + q_2 k_2 t} \quad (6)$$

Figure 4 shows the curves of the pseudosecond-order model for the single and binary dye adsorption systems. The kinetic parameters of the adsorption are presented in Table 2. It can be seen from Table 2 that the pseudosecond-order kinetic model has a higher correlation coefficient than the pseudofirst-order model for the different systems studied. All of these results indicate that the adsorption of AR183 and RB4 on WM in single and binary dye solutions followed the pseudosecond-order kinetic model. The pseudosecond-order kinetic model constants show that the adsorption rate of AR183 is higher than RB4 adsorption in both single and binary systems. The pseudosecond-order kinetic model is based on the assumption that the rate-limiting step may be chemical sorption or chemisorption involving valency forces through sharing or exchange of electrons between sorbent and sorbate.[33] The zero potential of WM has confirmed such an adsorption mechanism.

Adsorption Isotherms. Isotherms describe the equilibrium relationship between the concentration of an adsorbate on the solid phase and its concentration in the liquid phase at constant temperature. In general, the Langmuir and Freundlich models are commonly used to describe the adsorption process.[34,35]

The Langmuir isotherm model assumes the uniform energies of adsorption onto adsorbent surfaces. Furthermore, the Langmuir equation is based on the assumption of the existence of a

Table 2. Kinetic Parameters of Dye Adsorption in Single and Binary Systems

	pseudofirst-order kinetic model			pseudosecond-order kinetic model		
dye solution	q_e / mol·g^{-1}	k_1 / min^{-1}	r^2	q_e / mol·g^{-1}	k_2 / g·mol^{-1}·min^{-1}	r^2
AR183 (single system)	$9.34\cdot10^{-5}$	$7.23\cdot10^{-2}$	0.950	$9.03\cdot10^{-5}$	$8.84\cdot10^{2}$	0.999
RB4 (single system)	$6.42\cdot10^{-5}$	$6.15\cdot10^{-2}$	0.982	$7.53\cdot10^{-5}$	$7.09\cdot10^{2}$	0.998
AR183 (with RB4)	$5.30\cdot10^{-5}$	$5.41\cdot10^{-2}$	0.980	$6.89\cdot10^{-5}$	$5.66\cdot10^{2}$	0.997
RB4 (with AR183)	$3.34\cdot10^{-5}$	$2.70\cdot10^{-2}$	0.984	$4.95\cdot10^{-5}$	$4.80\cdot10^{2}$	0.998

Table 3. Adsorption Isotherm Parameters of Dye Adsorption in Single and Binary Systems

	Langmuir isotherm			Freundlich isotherm			binary Langmuir isotherm model				
dye solution	q_{max} / mol·g^{-1}	K_L / L·mol^{-1}	r_L^2	K_F / mol·g^{-1}	$1/n$	r_F^2	q_{max1} / mol·g^{-1}	K_{L1} / L·mol^{-1}	q_{max2} / mol·g^{-1}	K_{L2} / L·mol^{-1}	r_L^2
AR183 (single system)	$9.11\cdot10^{-5}$	$6.72\cdot10^{4}$	0.996	$1.11\cdot10^{-3}$	0.29	0.876					
RB4 (single system)	$7.33\cdot10^{-5}$	$4.08\cdot10^{4}$	0.998	$1.64\cdot10^{-3}$	0.36	0.950					
AR183 (with RB4)	$6.60\cdot10^{-5}$	$2.38\cdot10^{4}$	0.996	$1.58\cdot10^{-3}$	0.38	0.921	$7.43\cdot10^{-5}$	$6.72\cdot10^{4}$			0.985
RB4 (with AR183)	$5.16\cdot10^{-5}$	$1.21\cdot10^{4}$	0.997	$3.14\cdot10^{-3}$	0.52	0.953			$6.37\cdot10^{-5}$	$4.08\cdot10^{4}$	0.988

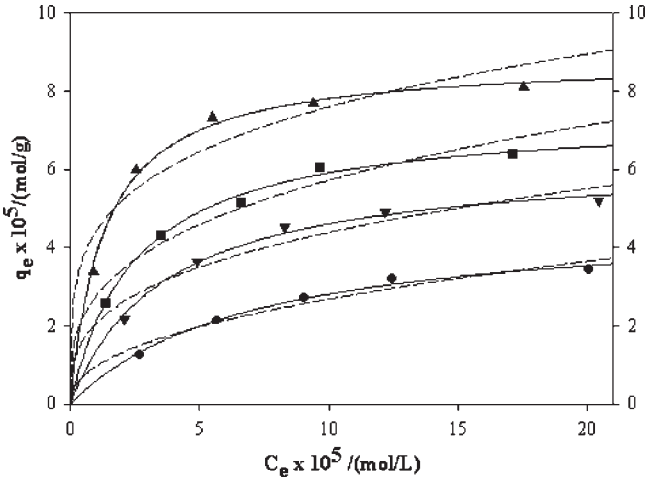

Figure 5. Adsorption isotherms for the adsorption of AR183 and RB4 from single and binary solutions [pH: 3; T: 298 K, adsorbent dosage: 1 g·L^{-1}; contact time: 60 min; agitation speed: 200 rpm; ▲, AR183 (single system); ■, RB4 (single system); ▼, AR183 (with RB4); ●, RB4 (with AR183); —, Langmuir isotherm model; – – –, Freundlich isotherm model].

monolayer coverage of the adsorbate at the outer surface of the adsorbent where all sorption sites are identical. The Langmuir equation[36] is given as follows:

$$q_e = \frac{q_{max} K_L C_e}{1 + K_L C_e} \tag{7}$$

$$\frac{1}{q_e} = \frac{1}{q_{max}} + \left(\frac{1}{q_{max} K_L}\right)\frac{1}{C_e} \tag{8}$$

where q_e is the equilibrium dye concentration on the adsorbent (mol·g^{-1}); C_e, the equilibrium dye concentration in solution (mol·L^{-1}); q_{max}, the monolayer capacity of the adsorbent (mol·g^{-1}); K_L, the Langmuir constant. Plots of $1/q_e$ versus $1/C_e$ give a straight line of slope $(1/q_{max}K_L)$ and intercept $(1/q_{max})$.

The Freundlich isotherm model equation[37] is expressed as:

$$q_e = K_F C_e^{1/n} \tag{9}$$

$$\ln q_e = \ln K_F + \frac{1}{n}\ln C_e \tag{10}$$

where q_e is the equilibrium dye concentration on the adsorbent (mol·g^{-1}); C_e, the equilibrium dye concentration in solution (mol·L^{-1}); K_F, the Freundlich constant. In this function, it is assumed that the sorbent has a surface with a nonuniform distribution of sorption heat. This equation was primarily proposed on a purely empirical basis for adsorption phenomena occurring on gas−solid interfaces, although it can be theoretically derived from an adsorption model in which the heat of adsorption varies exponentially with surface coverage.

The adsorption isotherm parameters calculated according to the Langmuir and Freundlich models for both single and binary systems are presented in Table 3. As shown in Figure 5, the adsorption isotherms were of the L-curve type even in the binary-dye system, similar to that of the single-dye system, indicating that the adsorption mechanisms did not change under the conditions of competition. The L-type nature of the curve indicates the higher affinity of the adsorbate for the adsorbent.[38] As seen in Table 3, a comparison of the experimental isotherm with the adsorption isotherm models revealed that the equilibrium data of single systems were well-fit to the Langmuir isotherm model as compared to the other isotherm model. The uptakes in binary system resulted in a decrease in AR183 and RB4 sorption by 27.55 % and 29.60 %, respectively, because these dyes compete with each other to a limited number of adsorption sites. The adsorption characteristics of both dyes are

probably associated with different sites of the adsorbent. Many investigators also observed a reduction in dye sorption in multidye systems.[39,40]

A binary Langmuir model[30] for two components was also applied to express the relationship between the quantity of the first component adsorbed and the concentration of the second component. This model assumes a homogeneous surface with respect to the energy of adsorption, no interaction between adsorbed species, and that all sites are equally available to all adsorbed species.

The competitive binary Langmuir model equations[30] are given as;

$$q_{e1} = \frac{q_{max1} K_{L1} C_{e1}}{1 + K_{L1} C_{e1} + K_{L2} C_{e2}} \quad (11)$$

$$q_{e2} = \frac{q_{max2} K_{L2} C_{e2}}{1 + K_{L1} C_{e1} + K_{L2} C_{e2}} \quad (12)$$

where q_{max1} and q_{max2} are the maximum adsorption capacity of adsorbates 1 and 2, respectively, and K_{L1} and K_{L2} are the individual Langmuir constants of adsorbates 1 and 2, respectively.

The experimental data in the binary systems were applied to the binary Langmuir equation, and the parameters obtained are given in Table 3. As shown in Table 3, the adsorption capacities of AR183 and RB4 were $7.43 \cdot 10^{-5}$ and $6.37 \cdot 10^{-5}$ mol·g^{-1}, respectively. The correlation coefficients for the binary Langmuir model in the binary system were lower than the correlation coefficients for the Langmuir isotherm model in the single dye systems. This can be explained that the competitive Langmuir model is under the same assumption with the pure component system; that is, the adsorbent surface is homogeneous and there is no interaction between the adsorbed molecules. These requirements are rarely accomplished in real systems because the effect of surface heterogeneity and interaction between sorbate molecules in the binary system are generally important. In this study, the adsorption of the anionic dyes in the binary system can be explained by the binary Langmuir isotherm model.

Adsorption Thermodynamics. Thermodynamic parameters reveal the feasibility and spontaneous nature of the adsorption process. The thermodynamic parameters, namely, the Gibbs energy change (ΔG), entropy change (ΔS), and enthalpy change (ΔH), were studied using the equilibrium constants at different temperatures [(293 to 323) K]. The adsorption equilibrium constant (K_c) can be calculated by the following equation;

$$K_c = \frac{C_{ad}}{C_{eq}} \quad (13)$$

C_{ad} is the amount of dye (mol) adsorbed on the adsorbent per liter (L) of the solution at equilibrium, and C_{eq} is the equilibrium concentration (mol·L^{-1}) of the dye in the solution. The Gibbs energy change (ΔG) of the adsorption is given by the following equation;

$$\Delta G = -RT \ln K_c \quad (14)$$

The relationship between equilibrium constant (K_c) and temperature (T) is expressed using the van't Hoff equation;

$$\ln K_c = \frac{\Delta S}{R} - \left(\frac{\Delta H}{R}\right)\frac{1}{T} \quad (15)$$

Adsorption enthalpy (ΔH) and entropy (ΔS) values were calculated from the slope and intercept of the linear plot ln K_c versus $1/T$ (Figure 6). The adsorption parameters are presented in Table 4. In the single systems, the negative values of ΔG indicate the overall adsorption processes are spontaneous. In the binary systems, the Gibbs energy (ΔG) increased to change to a positive value with rising temperature. This may be due to the interaction between the dyes on the solid surface, with nonequal competition attributed to the heterogeneity of adsorbent surface, and the system gained energy from an external source at high temperatures. The negative values of enthalpy (ΔH) confirmed an exothermic process, the nature of adsorption for both the single and binary systems. The negative values of entropy (ΔS) represented decreased randomness at the solid−liquid interface during the adsorption of dyes onto WM.

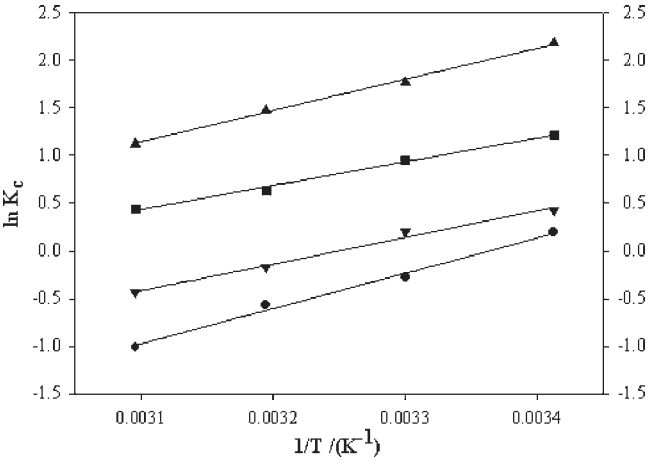

Figure 6. Plot of ln K_c vs $1/T$ for the estimation of thermodynamic parameters. ▲, AR183 (single system); ■, RB4 (single system); ▼, AR183 (with RB4); ●, RB4 (with AR183).

Fixed-Bed Column Studies. The breakthrough curves are very important characteristics for determining the operation and the dynamic response of an adsorption in a fixed-bed column. The breakthrough time (t_b) shows the time at which the outlet dye concentration reached the initial concentration, and the exhaustion time (t_e) represents the time at which the outlet dye concentration exceeded 95 % of the inlet dye concentration. The breakthrough curves were obtained for the adsorption of AR183 and RB4 on WM from single and binary dye solutions by varying the flow rate [(1, 3, and 5) mL·min^{-1}] with a constant bed height (6 cm) and inlet dye concentration (100 mg·L^{-1}). The column parameters are shown in Table 5. As the flow rate increased, the dye adsorption capacity and the breakthrough and exhaustion time were reduced, and the solute left the column before the equilibrium for both single and binary systems (Table 5 and Figure 7). This is attributed to the decrease in residence time of the dye molecule within the bed at higher flow rates. If intraparticle mass transfer controls the process, a slower flow rate is favored, and if external mass transfer controls the process, a higher flow rate decreases the film resistance.[41]

Figure 7 shows the breakthrough curves for single and binary dye adsorption systems at the flow rate of 1 mL·min^{-1}. In the single dye system, the breakthrough time of AR183 and RB4 occurred at (13.4 and 12.9) h, respectively. The column adsorption capacities for AR183 (91.02 mg·g^{-1}) was higher than that for RB4 (87.10 mg·g^{-1}). The results indicate that the column uptake for AR183 and RB4 was in agreement with the batch experimental data. In the binary system, the breakthrough time

Table 4. Thermodynamic Parameters of the Dye Adsorption in the Single and Binary Systems

dye solution	$\Delta G^o/(kJ\cdot mol^{-1})$				ΔH^o	ΔS^o	r^2
	293 K	303 K	313 K	323 K	$kJ\cdot mol^{-1}$	$J\cdot mol^{-1}\cdot K^{-1}$	
AR183 (single system)	−5.31	−4.47	−3.86	−3.02	−27.19	−74.78	0.997
RB4 (single system)	−2.97	−2.03	−1.43	−0.76	−24.10	−72.41	0.994
AR183 (with RB4)	−1.03	−0.50	0.44	1.18	−23.21	−77.44	0.989
RB4 (with AR183)	−0.48	0.71	1.49	2.71	−30.72	−103.34	0.993

Table 5. Column Parameters for the Single and Binary Dye Adsorption Using the Waste Materials

					Thomas model		
dye solution	flow rate	uptake	t_b	t_e	$k_{Th}\cdot 10^3$	q_o	r^2
	$mL\cdot min^{-1}$	$mg\cdot g^{-1}$	h	h	$L\cdot mg^{-1}\cdot h^{-1}$	$mg\cdot g^{-1}$	
AR183 (single system)	1	91.02	13.4	73.5	1.39	91.07	0.992
	3	82.90	9.6	51.5	2.03	82.98	0.991
	5	67.49	8.5	32.2	3.40	67.57	0.981
RB4 (single system)	1	87.10	12.9	65.4	1.69	87.14	0.991
	3	78.96	7.4	46.5	2.31	79.05	0.987
	5	62.09	6.6	27.6	3.96	62.18	0.973
AR183 (with RB4)	1	66.15	6.2	50.6	1.97	66.21	0.993
	3	58.86	4.6	36.3	2.76	59.04	0.974
	5	46.39	4.4	20.9	4.93	46.47	0.978
RB4 (with AR183)	1	55.12	7.8	43.4	2.42	55.18	0.987
	3	47.81	5.2	30.6	3.32	47.95	0.988
	5	39.45	3.1	17.9	5.83	39.57	0.974

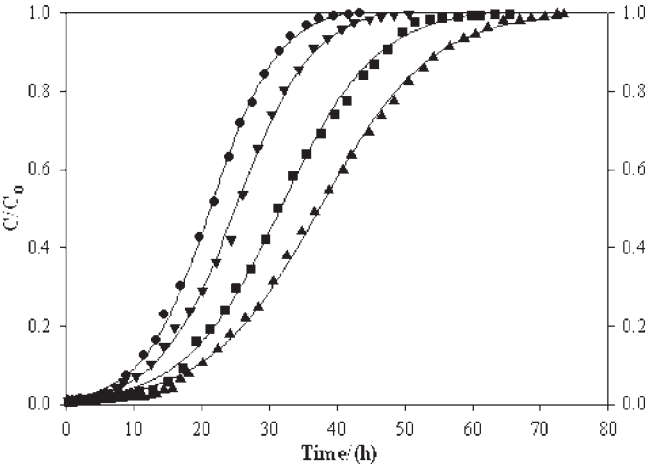

Figure 7. Breakthrough curves for the adsorption of AR183 and RB4 dyes from single and binary solutions [flow rate = 1 $mL\cdot min^{-1}$, inlet dye concentration C_o = 100 $mg\cdot L^{-1}$ (single system), C_o = (100 mg AR183 + 100 mg RB4)/L (binary system), bed height = 6 cm, pH = 3; ▲, AR183 (single system); ■, RB4 (single system); ▼, AR183 (with RB4); ●, RB4 (with AR183); —, Thomas model].

reduced to (6.2 and 7.8) h for AR183 and RB4, respectively. The breakthrough capacity of the dyes is higher in the case of the column process than the batch process. This is due to a continuously large concentration at the interface of the sorption zone as the adsorbate passes through the column, while the concentration gradient decreases with time in a batch process.

Different simple mathematical models have been developed to describe and possibly predict the dynamic behavior of column performance. One of these models used for continuous flow conditions is the Thomas model,[42] which can be given as;

$$\ln\left(\frac{C_o}{C_t} - 1\right) = \frac{k_{Th}q_o w}{Q} - k_{Th}C_o t \qquad (16)$$

where k_{Th} ($mL\cdot min^{-1}\cdot mg^{-1}$) is the Thomas model constant; q_o ($mg\cdot g^{-1}$) is the equilibrium dye adsorbed per g of the adsorbent; C_o ($mg\cdot L^{-1}$) is the inlet dye concentration; C_t ($mg\cdot L^{-1}$) is the outlet concentration at time t; W (g) the mass of adsorbent, and Q ($mL\cdot min^{-1}$) the flow rate. The plots of $\ln[C_o/C_t) - 1]$ versus time (t) give a straight line of slope (k_{Th}) and intercept (q_o) (figure not shown). The Thomas model parameters are presented in Table 5.

The Thomas model[42] assumes plug flow behavior in the bed and uses the Langmuir isotherm for equilibrium and second-order reversible reaction kinetics. This model is suitable for adsorption processes where external and internal diffusion limitations are absent.[42] It can be seen in Table 5, with an increase of the flow rate, that the value of k_{Th} increased, which indicates that the mass transport resistance decreases. As shown in Table 5, theoretical and experimental q_o values are in a good accordance with each other. Therefore, the adsorption process was fit well by the Thomas model.

■ CONCLUSIONS

This study reports the removal of AR183 and RB4 from single and binary solutions using WM in batch and fixed-bed column

dx.doi.org/10.1021/je100993m |J. Chem. Eng. Data 2011, 56, 508–516

processes. The adsorption was found to be significantly dependent on solution pH (3), adsorbent dosage (1 $g \cdot L^{-1}$), contact time (60 min), and temperature (298 K) in the batch system. Because of repulsion caused by each anionic dye molecule and competition in the binary solutions, the adsorption capacity of the single dye system was higher than that of the binary dye system for both batch and fixed-bed column adsorption processes. The pseudosecond-order kinetic model and the Langmuir isotherm were obtained to fit the experimental data. Thermodynamic parameters indicated exothermic and spontaneous reactions of adsorption for the single and binary systems. The negative values of entropy change showed a decrease in the degree of freedom of the adsorbed molecules. A series of column experiments revealed that the breakthrough time and exhaustion time decreased with an increase of flow rate. The Thomas model was used to describe the behavior of the column adsorption process, and it was found that the theoretical and experimental q_o values were in a good accordance with each other. The fixed-bed column experiments showed that WM can be efficiently and economically used as an adsorbent for the continuous removal of the textile dyes from single and multidye mixtures.

AUTHOR INFORMATION

Corresponding Author

*E-mail: shaobin.wang@curtin.edu.au.

REFERENCES

(1) Mittal, A.; Mittal, J.; Malviya, A.; Gupta, V. K. Removal and recovery of Chrysoidine Y from aqueous solutions by waste materials. *J. Colloid Interface Sci.* **2010**, *344*, 497–507.

(2) Garg, V. K.; Amita, M.; Kumar, R.; Gupta, R. Basic dye (methylene blue) removal from simulated wastewater by adsorption sawdust: a timber using Indian Rosewood industry waste. *Dyes Pigm.* **2004**, *63*, 243–250.

(3) Ozcan, A.; Oncu, E. M.; Ozcan, A. S. Kinetics, isotherm and thermodynamic studies of adsorption of Acid Blue 193 from aqueous solutions onto natural sepiolite. *Colloids Surf., A* **2006**, *277*, 90–97.

(4) Yener, J.; Kopac, T.; Dogu, G.; Dogu, T. Adsorption of Basic Yellow 28 from aqueous solutions with clinoptilolite and Amberlite. *J. Colloid Interface Sci.* **2006**, *294*, 255–264.

(5) Gupta, V. K.; Suhas; Ali, I.; Saini, V. K. Removal of rhodamine B, fast green, and methylene blue from wastewater using red mud, an aluminum industry waste. *Ind. Eng. Chem. Res.* **2004**, *43*, 1740–1747.

(6) Gupta, V. K.; Mohan, D.; Sharma, S.; Sharma, M. Removal of basic dyes (rhodamine B and methylene blue) from aqueous solutions using bagasse fly ash. *Sep. Sci. Technol.* **2000**, *35*, 2097–2113.

(7) Stephenson, R. J.; Duff, S. J. B. Coagulation and precipitation of a mechanical pulping effluent 0.1. Removal of carbon, colour and turbidity. *Water Res.* **1996**, *30*, 781–792.

(8) Mohan, N.; Balasubramanian, N.; Subramanian, V. Electrochemical treatment of simulated textile effluent. *Chem. Eng. Technol.* **2001**, *24*, 749–753.

(9) Wang, S. A Comparative study of Fenton and Fenton-like reaction kinetics in decolourisation of wastewater. *Dyes Pigm.* **2008**, *76*, 714–720.

(10) Ling, S. K.; Wang, S.; Peng, Y. Oxidative degradation of dyes in water using Co^{2+}/H_2O_2 and Co^{2+}/peroxymonosulfate. *J. Hazard. Mater.* **2010**, *178*, 385–389.

(11) Sojka-Ledakowicz, J.; Zylla, R.; Mrozinska, Z.; Pazdzior, K.; Klepacz-Smolka, A.; Ledakowicz, S. Application of membrane processes in closing of water cycle in a textile dye-house. *Desalination* **2010**, *250*, 634–638.

(12) You, S. J.; Damodar, R. A.; Hou, S. C. Degradation of Reactive Black 5 dye using anaerobic/aerobic membrane bioreactor (MBR) and photochemical membrane reactor. *J. Hazard. Mater.* **2010**, *177*, 1112–1118.

(13) Wang, S. B.; Boyjoo, Y.; Choueib, A.; Zhu, Z. H. Removal of dyes from aqueous solution using fly ash and red mud. *Water Res.* **2005**, *39*, 129–138.

(14) Wang, S. B.; Boyjoo, Y.; Choueib, A.; Ng, E.; Wu, H. W.; Zhu, Z. H. Role of unburnt carbon in adsorption of dyes on fly ash. *J. Chem. Technol. Biotechnol.* **2005**, *80*, 1204–1209.

(15) Ali, I.; Gupta, V. K. Advances in water treatment by adsorption technology. *Nat. Protocols* **2007**, *1*, 2661–2667.

(16) Gupta, V. K.; Carrott, P. J. M.; Ribeiro Carrott, M. M. L.; Suhas Low cost adsorbents: Growing approach to wastewater treatment - A review. *Crit. Rev. Environ. Sci. Technol.* **2009**, *39*, 783–842.

(17) Gupta, V. K.; Suhas Application of low cost adsorbents for dye removal - A review. *J. Environ. Manag.* **2009**, *90*, 2313–2342.

(18) Oei, B. C.; Ibrahim, S.; Wang, S. B.; Ang, H. M. Surfactant modified barley straw for removal of acid and reactive dyes from aqueous solution. *Bioresour. Technol.* **2009**, *100*, 4292–4295.

(19) Wang, S. B.; Ang, H. M.; Tade, M. O. Novel applications of red mud as coagulant, adsorbent and catalyst for environmentally benign processes. *Chemosphere* **2008**, *72*, 1621–1635.

(20) Janos, P.; Buchtova, H.; Ryznarova, M. Sorption of dyes from aqueous solutions onto fly ash. *Water Res.* **2003**, *37*, 4938–4944.

(21) Wang, S. B.; Wu, H. W. Environmental-benign utilisation of fly ash as low-cost adsorbents. *J. Hazard. Mater.* **2006**, *136*, 482–501.

(22) Ramakrishna, K. R.; Viraraghavan, T. Use of slag for dye removal. *Waste Manage.* **1998**, *17*, 483–488.

(23) Wang, S. B.; Peng, Y. L. Natural zeolites as effective adsorbents in water and wastewater treatment. *Chem. Eng. J.* **2010**, *156*, 11–24.

(24) Jain, A. K.; Gupta, V. K.; Bhatnagar, A.; Suhas Utilization of industrial waste products as adsorbents for the removal of dyes. *J. Hazard. Mater.* **2003**, *101*, 31–42.

(25) Olgun, A.; Atar, N. Equilibrium and kinetic adsorption study of Basic Yellow 28 and Basic Red 46 by a boron industry waste. *J. Hazard. Mater.* **2009**, *161*, 148–156.

(26) Atar, N.; Olgun, A. Removal of acid blue 062 on aqueous solution using calcinated colemanite ore waste. *J. Hazard. Mater.* **2007**, *146*, 171–179.

(27) Atar, N.; Olgun, A. Removal of basic and acid dyes from aqueous solutions by a waste containing boron impurity. *Desalination* **2009**, *249*, 109–115.

(28) Vijayaraghavan, K.; Won, S. W.; Yun, Y. S. Single- and dual-component biosorption of reactive black 5 and reactive orange 16 onto polysulfone-immobilized esterified Corynebacterium glutamicum. *Ind. Eng. Chem. Res.* **2008**, *47*, 3179–3185.

(29) Vijayaraghavan, K.; Yun, Y. S. Competition of Reactive red 4, Reactive orange 16 and Basic blue 3 during biosorption of Reactive blue 4 by polysulfone-immobilized Corynebacterium glutamicum. *J. Hazard. Mater.* **2008**, *153*, 478–486.

(30) Choy, K. K. H.; Porter, J. F.; McKay, G. Langmuir isotherm models applied to the multicomponent sorption of acid dyes from effluent onto activated carbon. *J. Chem. Eng. Data* **2000**, *45*, 575–584.

(31) Mance, G.; O'Donnell, A. R.; Smith, P. R. *Proposed Environmental Quality Standards for List II Substances in Water*; Water Research Centre: Swindon, U.K., 1988.

(32) Lagergren, S. Zur theorie der sogenannten adsorption gelöster stoffe, Kungliga Svenska Vetenskapsakademiens. *Handlingar* **1898**, *24*, 1–39.

(33) Ho, Y. S.; McKay, G. Kinetic models for the sorption of dye from aqueous solution by wood. *Process Saf. Environ. Prot.* **1998**, *76*, 183–191.

(34) Shen, D. Z.; Fan, J. X.; Zhou, W. Z.; Gao, B. Y.; Yue, Q. Y.; Kang, Q. Adsorption kinetics and isotherm of anionic dyes onto organo-bentonite from single and multisolute systems. *J. Hazard. Mater.* **2009**, *172*, 99–107.

(35) Mittal, A.; Krishnan, L.; Gupta, V. K. Removal and recovery of malachite green from wastewater using an agricultural waste material, de-oiled soya. *Sep. Purif. Technol.* **2005**, *43*, 125–133.

(36) Langmuir, I. The adsorption of gases on plane surfaces of glass, mica and platinum. *J. Am. Chem. Soc.* **1918**, *40*, 1361–1403.
(37) Freundlich, H. M. F. Uber die adsorption in Losungen. *Z. Phys. Chem.* **1906**, *57*, 385–470.
(38) Giles, C. H.; Smith, D.; Huitson, A. General treatment and classification of solute adsorption-isotherm. 1. theoretical. *J. Colloid Interface Sci.* **1974**, *47*, 755–765.
(39) Turabik, M. Adsorption of basic dyes from single and binary component systems onto bentonite: Simultaneous analysis of Basic Red 46 and Basic Yellow 28 by first order derivative spectrophotometric analysis method. *J. Hazard. Mater.* **2008**, *158*, 52–64.
(40) Al-Degs, Y.; Khraisheh, M. A. M.; Allen, S. J.; Ahmad, M. N.; Walker, G. M. Competitive adsorption of reactive dyes from solution: Equilibrium isotherm studies in single and multisolute systems. *Chem. Eng. J.* **2007**, *128*, 163–167.
(41) Vijayaraghavan, K.; Jegan, J.; Palanivelu, K.; Velan, M. Removal of Nickel(II) ions from aqueous solution using crab shell particles in a packed bed up-flow column. *J. Hazard. Mater.* **2004**, *113*, 225–232.
(42) Thomas, H. C. Heterogeneous ion exchange in a flowing system. *J. Am. Chem. Soc.* **1944**, *66*, 1664–1666.